Fig. 1. Heart; Vervet monkey. Heart revealed slight dilatation with various sized pale white spots on the surface. Bar = 1 cm.

Japan) with or without potassium permanganate (PPM). Positive reactions for Congo red and DFS were confirmed by apple green birefringence under polarizing microscope. Furthermore, some deparaffinized sections were immunostained using rabbit polyclonal antibodies against Aβ 1–42 (Aβ42; Chemicon, Temecula, CA; 1:100), amyloid P component (AP; DAKO, Glostrup, Denmark; 1:300), apolipoprotein E (apoE; DAKO; 1:1000), calcitonin (IBL, Takasaki, Japan; 1:400), kappa light chains (κAL; DAKO; 1:20000), lambda light chains (λAL; DAKO; 1:40000), and TTR (DAKO; 1:100) and using mouse monoclonal antibodies against amyloid A (AA; Novocastra, Newcastle, UK; 1:100) and IAPP (Serotec, Raleigh, NC; 1:100). Sections immunostained for Aβ42 were pretreated with 99% formic acid for 10 minutes. The remaining immunostains used pretreatment with citrate buffer (pH 6.0, 121°C, 10 min). These sections were further reacted with horseradish peroxidase-conjugated secondary mouse and rabbit immunoglobulins (EnVision+ System, DAKO) and then visualized with 3,3′-diaminobenzidine tetrahydrochloride (DAB).

At necropsy, the heart revealed slight dilatation of both ventricles with thinning of the right ventricular free wall. The surface of the heart was reddish brown with pale white spots (Fig. 1). The brain and pancreas showed slight atrophy.

Myocardium and stroma were multifocally replaced by hyaline material deposits, mainly in the free wall of the ventricles (Fig. 2). Hyaline deposits were observed regardless of the area in the heart, such as subendocardium or subepicardium and right or left wall. They showed uniform pale pink staining with hematoxylin and eosin in the extracellular stroma among the heart muscle fibers (Fig. 3). These hyaline deposits were positive for DFS and Congo red (Fig. 4, Table 1), and their reactions were resistant to PPM (data not shown). DFS and Congo red stained the hyaline deposits; however, DFS showed less nonspecific background than did Congo red. Apple green birefringence corresponding to their hyaline deposits was observed by both DFS and Congo red under polarizing microscope (data not shown). The intensity of birefringence was stronger with Congo red than with DFS (data not shown). Moreover, in the heart, DFS- and Congo red–positive deposits were observed in the external tunica of some arterioles. These cardiac amyloids were immunohistochemically positive for antibodies against TTR, apoE, and AP (Fig. 5, Table 1). The intensity of TTR immunoreactivity was most significant. Moreover, immunoreactivity of TTR as well as of apoE was greater than that of AP. Heart muscle fibers adjoining the amyloid lesions showed necrotic or atrophic changes (Fig. 3).

Hyaline deposits were found mainly in the stromal connective tissues (fibrous and adipose tissues) and external tunic of the blood vessels. Moreover, faint deposits were observed in the peripheral nerves of the thyroid gland, tonsil, salivary glands, thymus, prostate gland, lymph nodes, and skeletal muscles (Table 1). As for mucosal organs, the deposits were found in lamina propria of the tongue, trachea, esophagus, stomach, intestines, and urinary bladder; submucosal layers of the stomach and intestines; muscular layer of the intestines and urinary bladder; and serosa of the trachea and esophagus (Table 1). Furthermore, hyaline deposits in the lungs were found in the alveolar walls, bronchial wall, and external tunica of arterioles (Table 1). In the kidneys, the deposits were detected in the renal pelvis and external tunica of the arcuate arteries (Table 1). In these organs, severe deposits were found in the thyroid gland, tongue, esophagus, and stomach; moderate deposits in the tonsil, thymus, lungs, intestines, and skeletal muscles; and weak deposits in the salivary glands, trachea, kidneys, urinary bladder, and lymph nodes. These deposits were positive for DFS and Congo red (Table 1) but resistant to PPM and revealed apple green birefringence under polarizing microscope (data not shown). These were immunohistochemically positive for antibodies against TTR, apoE, and AP (Table 1). The intensity of immunoreactivity was stronger for TTR and apoE than for AP. Furthermore, TTR-positive but DFS- and Congo red–negative lesions were detected in the external tunica of blood vessels of the testes. Reactivity for DFS and Congo red and immunoreactivity of TTR, apoE, and AP were not detected in the liver, spleen, pituitary, and adrenal gland (Table 1). Thus, based on histochemical and immunohistochemical characteristics of cardiac and other amyloids, systemic amyloidosis characterized by the deposition of amyloid fibrils containing TTR was confirmed.

The second type of hyaline deposit, such as neuritic senile plaques (SPs), was observed in the cerebral cortices. DFS and Congo red detected not only some neuritic SPs but also deposits consistent with cerebral amyloid angiopathy (CAA) (Table 1), as found previously in vervet and cynomolgus monkeys.[4,5] This type of amyloid was resistant to PPM and revealed apple green birefringence under polarizing microscope (data

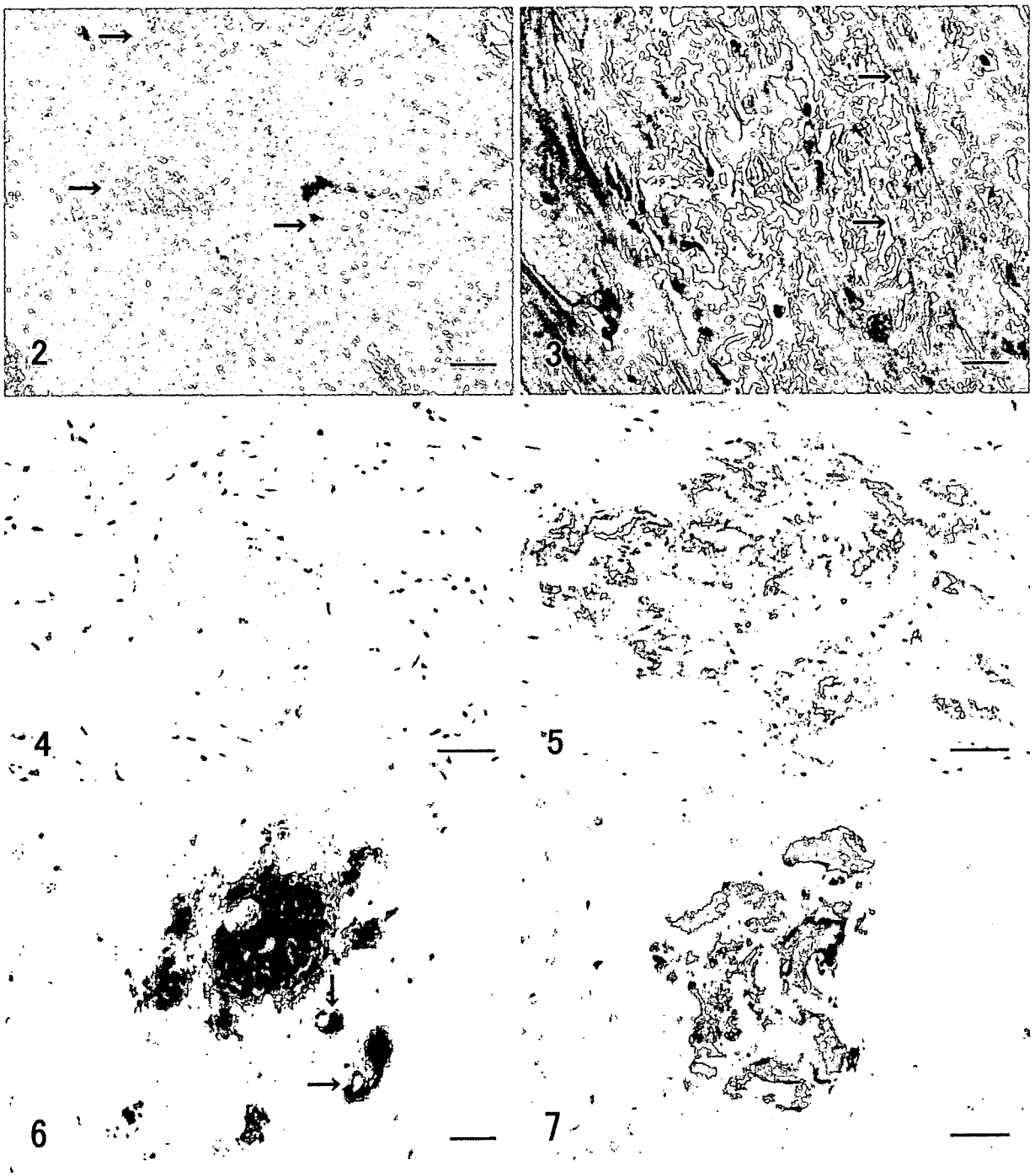

Fig. 2. Heart; vervet monkey. Hyaline deposits (arrows) were multifocally found in the heart wall. HE. Bar = 200 μm.

Fig. 3. Heart; vervet monkey. Hyaline materials showed uniform pale pink staining, and the surrounding muscle fibers revealed atrophic and necrotic changes (arrows). HE. Bar = 20 μm.

Fig. 4. Heart; vervet monkey. Hyaline materials were positive for direct fast scarlet (DFS). DFS. Bar = 50 μm.

Fig. 5. Heart; vervet monkey. Amyloid deposits were immunohistochemically positive for antibodies against transthyretin. Immunoperoxidase method, hematoxylin counterstain. Bar = 50 μm.

Fig. 6. Cerebrum; vervet monkey. Cerebral amyloid deposits, such as neuritic senile plaques and capillary-cerebral amyloid angiopathy (arrows), were immunohistochemically positive for antibodies against amyloid β protein. Immunoperoxidase method, hematoxylin counterstain. Bar = 20 μm.

Fig. 7. Pancreas; vervet monkey. Islet amyloid deposits were immunohistochemically positive for antibodies against islet amyloid polypeptide (IAPP). Immunoperoxidase method, hematoxylin counterstain. Bar = 20 μm.

Table 1. Histochemical and immunohistochemical features of amyloid depositions in various organs and tissues of an aged vervet monkey.

Organ or Tissue	DFS*	Congo Red	TTR	Aβ	IAPP	apoE	AP	Notes
Brain	++	+	−	+++	−	++	+	Senile plaques and amyloid angiopathy
Pituitary	−	−	−	−	−	−	−	
Thyroid	+++	++	+++	−	−	+++	+++	Parafollicular areas
Parathyroid	−	−	−	−	−	−	−	
Tongue	+++	+++	+++	−	−	+++	+++	Tunica propria, stroma, and blood vessels
Tonsil	++	+	++	−	−	+++	++	Stroma and adjoining connective tissues
Salivary	+	+	+	−	−	+	+	Stroma, blood vessels, and adjoining connective tissues
Trachea	+	+	++	−	−	+	+	Tunica propria and serosa
Esophagus	+++	+++	+++	−	−	+++	+++	Tunica propria, muscle layer, and serosa
Heart	+++	+++	+++	−	−	+++	+++	Myocardium and blood vessels
Thymus	++	++	+++	−	−	+++	++	Stroma and adjoining connective tissues
Lungs	++	++	+++	−	−	+++	+++	Alveolar and bronchus walls and blood vessels
Stomach	+++	+++	+++	−	−	+++	++	Tunica propria, submucosal and muscle layer, and blood vessels
Intestines	++	++	+++	−	−	+++	++	Tunica propria, muscle layer, and blood vessels
Pancreas	++	++	−	−	+++	+++	++	Islets
Liver	−	−	−	−	−	−	−	
Gall bladder	−	−	−	−	−	−	−	
Spleen	−	−	−	−	−	−	−	
Kidneys	+	+	+	−	−	+	+	Renal pelvis and arcuate arteries
Adrenal	−	−	−	−	−	−	−	
Testes	−	−	+	−	−	−	−	Blood vessels
Prostate	+++	+++	+++	−	−	+++	+++	Stroma and blood vessels
Urinary bladder	+	+	+	−	−	+	+	Muscle layer and blood vessels
Lymph nodes	+	+	++	−	−	++	+	Stroma, blood vessels, and adjoining connective tissues
Skeletal muscle	++	++	++	−	−	++	+	Stroma and blood vessels
Sciatic nerve	−	−	−	−	−	−	−	
Bone	−	−	−	−	−	−	−	
Bone marrow	−	−	−	−	−	−	−	
Skin	NT	NT	NT	NT	NT	NT	NT	

* DFS = direct fast scarlet; TTR = transthyretin; Aβ = amyloid β protein; IAPP = islet amyloid polypeptide; apoE = apolipoprotein E; AP = amyloid P component.

+++ = strong positive; ++ = moderate positive; + = weak positive; − = negative; NT = not tested.

not shown). Furthermore, SPs and CAA were immunohistochemically labeled using antibodies against Aβ42, apoE, and AP (Fig. 6, Table 1). The intensity of immunoreactivity was stronger with Aβ42 and apoE than with AP. Diffuse plaques, found previously in cynomolgus monkeys,[5] were not found in the present case. This amyloid derived from Aβ was not deposited in the other organs (Table 1).

The third type of hyaline deposit was found in the expanded stromal areas of islets of the pancreas. This was positive for Congo red and DFS and resistant to PPM (Table 1) and showed apple green birefringence under polarizing microscope (data not shown). This amyloid was immunohistochemically positive for antibodies against IAPP, apoE, and AP (Fig. 7, Table 1). The intensity of immunoreactivity was stronger with

IAPP and apoE than with AP. The islets, where abundant amyloid was deposited, had a reduced number of islet cells. This IAPP-derived amyloid was not detected from any other organ (Table 1).

Finally, all the 3 types of hyaline deposits were immunohistochemically negative for antibodies against AA, calcitonin, κAL, and λAL (Table 1).

Although there is no information about amino acid sequences of TTR, Aβ, and IAPP in vervet monkeys, the sequences in human are 93.1%, 100%, and 94.6% homology (BAC20609 and XP_001098180),[11] respectively, against those in macaque monkeys and vervet monkeys, who belong taxonomically to *Cercopithecus*. Antibodies to TTR and Aβ used in the present study have reacted with each amyloid lesion, that is, cardiac amyloid in SSA and SPs in AD, consisting of intact mature amyloid in human.[8,12] The immunoreactivities of humans were absolutely corresponding to that of this vervet monkey. According to these facts, we assumed that these antibodies recognized suitable TTR and Aβ amyloid lesions in vervet monkeys, as well as humans. On the other hand, as for IAPP, detail immunohistochemical information of an antibody to IAPP 7–17 residue used in this study has not been described, while similar antibodies to IAPP 8–17 residue reacted well with intact islet amyloid in humans and cats.[6] The immunoreactivity of an antibody to IAPP 8–17 was consistent with that of an antibody to IAPP 7–17. Those IAPP residues are conserved between various mammalian species, and IAPP 8–20 is known as the second major constituent of islet amyloid.[5] Therefore, we assumed that the antibody to IAPP used in this study reacted precisely with intact islet amyloid of this monkey species.

SSA is one of the common systemic amyloidoses in humans, occurring in 25% of people who are older than 80 years.[15] SSA has been previously called cardiac amyloidosis because it shows cardiac symptoms, such as heart failure and/or arrhythmia, due to severe amyloid deposition in the heart.[15] As for histopathologic characteristics of SSA in humans, the organ most severely affected by amyloid deposition is the heart, while deposition is also found in the other systemic organs. On the other hand, there are few amyloid deposits in the liver, spleen, and kidney, except the renal pelvis, which are frequent organs for other types of systemic amyloidoses, such as AA or AL amyloidosis.[15] These histopathologic features in humans are consistent with those in the vervet monkey. Furthermore, clinical symptoms, such as arrhythmia, and biochemical aspects of the amyloid precursor, such as TTR and not AA or AL, in humans, correspond to the characteristics in the vervet monkey.[14] Another manifestation of TTR amyloid deposition is familial or hereditary TTR amyloidosis, which is known as familial amyloid polyneuropathy (FAP).[15] FAP patients with a variant TTR reveal onset of cardiac symptoms and severe systemic TTR amyloidosis usually the third decade of life, with deposits especially prominent in the heart and peripheral nervous system.[13] Because there is no information for TTR amino acid sequence and its mutant in vervet monkeys, the hereditary aspect of TTR amyloidosis could not be considered in the present study. However, the clinical, histologic, and immunohistochemical features suggest that the monkey suffered from SSA and not FAP, because the monkey was very old (a 29-year-old monkey corresponds nearly to an 85-year-old human) and because amyloid was deposited exclusively in the heart rather than in the peripheral nerves.

Teng and colleagues[14] reported that transgenic mice overexpressing human wild-type *TTR* gene revealed predominant deposits of TTR-positive and DFS-negative materials in the heart and kidney. This type of deposit is consistent with the deposits in the testes of the vervet monkey in this study. Namely, the deposits in TTR transgenic mice and this vervet monkey may be considered immature materials before amyloid fibril formation.[14]

Cerebral amyloidosis consisting of Aβ is an aging-related amyloidosis, although it occurs earlier and is significantly developed in Alzheimer's disease.[6,8] SPs and CAA as histopathologic hallmarks in Alzheimer's disease also appear in aged nonhuman primates.[7] SPs in cynomolgus monkeys are morphologically classified into neuritic and diffuse plaques; the neuritic plaques are more frequently observed than the diffuse ones, whereas CAA is more frequently found in capillaries than in meningeal arterioles.[7] Findings of abundant neuritic plaques and predominant capillary CAA rather than meningeal CAA have been described previously, in the first study of SPs and CAA in a vervet monkey.[4] The characteristics of SPs and CAA in the present study are consistent with the previous studies of cynomolgus monkeys.[7]

Islet amyloidosis consisting of IAPP often appears as one of the aging-related changes in aged primates including humans,[3] while this amyloid deposition is accelerated in diabetes mellitus.[13] Because the vervet monkey did not have any history for diabetes, possibilities are considered that the islet amyloid deposition in this monkey likely occurred as an aging-related change and that degrading insulin secretion in the absence of fasting hyperglycemia was associated with an increase of IAPP aggregation and the onset of islet amyloidosis.[3] This type of amyloid deposition has been previously reported in various primate species, that is, humans and macaque monkeys.[10,13] Morphologic and immunohistochemical characteristics of islet amyloidosis in vervet monkey are consistent with those in other primate species.[10]

ApoE and AP are often colocalized with various types of amyloid precursors, such as Aβ, prion protein, AA, and IAPP[7,9,13] and accelerate in vitro fibril formation of the amyloids.[1] Although in vitro data on the correlation between apoE and TTR have not been confirmed previously, the colocalization of apoE in the TTR amyloid portion suggests that TTR amyloid deposition might be accelerated by apoE and AP, as well as other types of amyloids.[13] In summery, 3 different aging-related amyloidoses were found in an

aged vervet monkey. TTR amyloidosis has only been reported in SAMP mice,[2] while this is the first spontaneous case report on TTR amyloidosis in mammalian species, other than humans and experimental animals with a special genetic background.

Acknowledgement

The authors thank Ms. Chieko Ohno for her technical help.

References

1 Hass S, Fresser F, Kochl S, Beyreuther K, Utermann G, Baier G: Physical interaction of ApoE with amyloid precursor protein independent of the amyloid Aβ region in vitro. J Biol Chem **273**:13892–13897, 1998

2 Higuchi K, Naiki H, Kitagawa K, Hosokawa M, Takeda T: Mouse senile amyloidosis: ASSAM amyloidosis in mice presents universally as a systemic age-associated amyloidosis. Virchows Arch B Cell Pathol Incl Mol Pathol **60**:231–238, 1991

3 Hull RL, Westermark GT, Westermark P, Kahn SE: Islet amyloid: a critical entity in the pathogenesis of type 2 diabetes. J Clin Endocrinol Metab **89**:3629–3643, 2004

4 Lemere CA, Beierschmitt A, Iglesias M, Spooner ET, Bloom JK, Leverone JF, Zheng JB, Seabrook TJ, Louard D, Li D, Selkoe DJ, Palmour RM, Ervin FR: Alzheimer's disease Aβ vaccine reduces central nervous system Aβ levels in a non-human primate, the Caribbean vervet. Am J Pathol **165**:283–297, 2004

5 Mazor Y, Gilead S, Benhar I, Gazit E: Identification and characterization of a novel molecular-recognition and self-assembly domain within the islet amyloid polypeptide. J Mol Biol **322**:1013–1024, 2002

6 Ma Z, Westermark GT, Johnson KH, O'Brien TD, Westermark P: Quantitative immunohistochemical analysis of islet amyloid polypeptide (IAPP) in normal, impaired glucose tolerant, and diabetic cats. Amyloid **5**:255–256, 1998

7 Nakamura S, Kiatipattanasakul W, Nakayama H, Ono F, Sakakibara I, Yoshikawa Y, Goto N, Doi K: Immunohistochemical characteristics of the constituents of senile plaques and amyloid angiopathy in aged cynomolgus monkeys. J Med Primatol **25**:294–300, 1996

8 Nagele RG, D'Andrea MR, Anderson WJ, Wang HY: Intracellular accumulation of β-amyloid$_{1-42}$ in neurons is facilitated by the alpha 7 nicotinic acetylcholine receptor in Alzheimer's disease. Neuroscience **110**:199–211, 2002

9 Namba Y, Tomonaga M, Kawasaki H, Otomo E, Ikeda K: Apolipoprotein E immunoreactivity in cerebral amyloid deposits and neurofibrillary tangles in Alzheimer's disease and kuru plaque amyloid in Creutzfeldt-Jakob disease. Brain Res **541**:163–166, 1991

10 O'Brien TD, Wagner JD, Litwak KN, Carlson CS, Cefalu WT, Jordan K, Johnson KH, Butler PC: Islet amyloid and islet amyloid polypeptide in cynomolgus macaques (*Macaca fascicularis*): an animal model of human non-insulin-dependent diabetes mellitus. Vet Pathol **33**:479–485, 1996

11 Podlisny MB, Tolan DR, Selkoe DJ: Homology of the amyloid β protein precursor in monkey and human supports a primate model for β amyloidosis in Alzheimer's disease. Am J Pathol **138**:1423–1435, 1991

12 Sawabe M, Hamamatsu A, Ito T, Arai T, Ishikawa K, Chida K, Izumiyama N, Honma N, Takubo K, Nakazato M: Early pathogenesis of cardiac amyloid deposition in senile systemic amyloidosis: close relationship between amyloid deposits and the basement membranes of myocardial cells. Virchows Arch **442**:252–257, 2003

13 Sipe JP: 2005 Amyloid Proteins, 1st ed., pp. 3–27, pp. 180–181, pp. 385–406, pp. 732–742. WILEY-VCH, Weinheim, Germany, 2005

14 Teng MH, Yin JY, Vidal R, Ghiso J, Kumar A, Rabenou R, Shah A, Jacobson DR, Tagoe C, Gallo G, Buxbaum J: Amyloid and nonfibrillar deposits in mice transgenic for wild-type human transthyretin: a possible model for senile systemic amyloidosis. Lab Invest **81**:385–396, 2001

15 Westermark P, Bergstrom J, Solomon A, Murphy C, Sletten K: Transthyretin-derived senile systemic amyloidosis: clinicopathologic and structural considerations. Amyloid **10**(Suppl 1): 48–54, 2003

Request reprints from Shinichiro Nakamura, Research Center for Animal Medical Science, Shiga University of Medical Science, Seta-Tsukinowa-Cho, Ohtsu, Shiga 520-2192 (Japan). E-mail: snakamur@belle.shiga-med.ac.jp.